THE JOURNAL OF PHYSICAL CHEMISTRY C

Article

pubs.acs.org/JPCC

Comparison of the Surface and Subsurface Oxygen Reactivity and Dynamics with CO Adsorbed on Rh(111)

K. D. Gibson, D. R. Killelea, and S. J. Sibener*

The James Franck Institute and Department of Chemistry, The University of Chicago, 929 E. 57th Street, Chicago, Illinois 60637, United States

ABSTRACT: The translational and angular intensity dependence of CO_2 produced from the reaction of CO with an initial oxygen coverage of 0.5 ML $\leq \Theta_O \leq$ 1.6 ML on Rh(111) at a surface temperature of 450 K was measured. This range of coverages goes from only surface absorbed O to both adsorbed and selvedge absorbed O. The measured CO_2 translational energy is independent of Θ_O and is larger than steady-state experiments [Colonell et al. *J. Chem. Phys.* **1995**, *103*, 6677], which were done at lower O coverages, but follows the trend that higher Θ_O leads to faster CO_2. The angular dependence of the intensity is well-described by a sharply peaked function of the form $I = a\cos^n(\theta) + (1 - a)\cos(\theta)$, with $a = 0.6$ and $n = 8.6$. Again, this was consistent with the previous steady-state results. These observations point to a similar reaction geometry regardless of Θ_O; the measured dynamical parameters are independent of whether or not some of the O is subsurface and suggest that absorbed oxygen in the selvedge acts only as a reservoir for replenishing reagent as it is consumed.

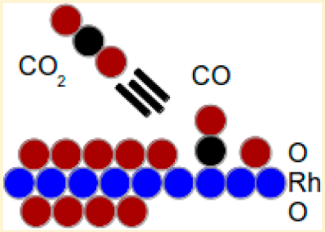

INTRODUCTION

The catalytic activity of metal surfaces is technologically important, and many techniques for studying the heterogeneous catalysis of gaseous species have been developed in an effort to understand the fundamental reaction mechanisms.[1−9] These techniques span a tremendous pressure range from ultrahigh vacuum (UHV) (~10^{-10} Torr) to many Torr. Often, the information obtained in experiments done in different pressures regimes is complementary, but a particular approach can only be implemented in a narrow window at one end of the pressure range. For instance, it would be difficult to measure the speed and angular distribution of desorbing reaction products at an ambient pressure of 10 Torr (mean free path much less than a mm), but the measurements are possible at 10^{-10} Torr (mean free path on the order of a km). Likewise, if the sticking coefficient is low, it is difficult to achieve high reactant concentrations on the surface at low pressures, but high concentrations occur at high pressures as a result of the larger reactant flux.

Often, it is the reactions at the higher pressures that are of the most interest because industrial processes take place under many atmospheres of pressure. Furthermore, environmentally important chemistry also takes place at the higher end of the pressure range of the experiments. But many techniques for elucidating the dynamics of the reactions work best at very low pressures. One of the major challenges facing surface science is reconciling the so-called "pressure gap", where measurements at one end of the pressure range seem to contradict those made at the other end. This is not a gap in phenomena as much as it is a gap in our understanding of the fundamental properties of reactions on metal surfaces. There are many examples where high- and low-pressure measurements have been reconciled; examples of the blending of low- and high-pressure measurements are given by the Goodman group[4,5,10] for CO oxidation and Stoltze and Nørskov[11] for ammonia synthesis.

The energy and angle at which the desorbing products of surface reactions, measurements made under UHV conditions, can give insight into the dynamics of the reaction.[1−3] The direction and energy of the reaction products relative to the surface normal provides key information on the orientation of the transition state and where the reaction takes place on stepped surfaces. Measuring how the energy liberated during the reaction is partitioned into the products yields valuable insight into the reaction mechanism.

In this paper, we will show results for the oxidation of CO on Rh(111). The experiments were done with surface concentrations of ab- and adsorbed oxygen between 0.5 and 1.6 monolayers (ML = $1.6 \times 10^{15}/cm^2$). This is a continuation of our earlier work on the same system.[12,13] These earlier experiments measured both the translational energy and the intensity of the desorbing CO_2 as a function of scattering angle (θ, measured from the surface normal) for surface temperatures between 450 and 1000 K. The measurements were done under UHV conditions utilizing simultaneous molecular beam dosing of the reactants but were only able to achieve low surface oxygen concentration ($\Theta_O \leq$ 0.3 ML). In the experiments described in this paper, we first load the surface with O and then expose it to a CO beam; this allows us to look at CO_2 production under much more oxidizing conditions. Further, we do these experiments at an elevated surface temperature (450 K) in an attempt to simulate normal catalytic conditions.

Under UHV conditions, the highest easily attained coverage of adsorbed O when using O_2 dosing is 0.5 ML.[14−17] Higher

Received: May 4, 2014
Revised: June 14, 2014
Published: June 27, 2014

dx.doi.org/10.1021/jp504369z | *J. Phys. Chem. C* 2014, 118, 14977−14982

coverages are only attained after large exposures well above room temperature.[18−21] Another method to achieve high Θ_O on Rh(111), and with much smaller exposures, is to use NO_2 dosing.[16,19] For 0.5 ML < $\Theta_O \leq$ 1.0 ML, it is not entirely clear whether the oxygen atoms are all adsorbed or if some are absorbed. Köhler et al.[21] determined that surface structures having an Θ_O of 2/3 or 3/4 were possible at 400 K. Gibson et al.[17] were able to grow a stable (1×1) adsorbed overlayer using O atom dosing. However, as inferred by He diffraction measurements, some probably migrated below the surface within 5 min at temperatures above 400 K. Wider et al.,[18] using X-ray photoelectron diffraction, determined that when there was ∼0.83 ML of adsorbed O, there was ∼0.05 ML of absorbed O. Ganduglia-Pirovano et al.[22,23] calculated that the (1×1) overlayer will form before any oxygen is incorporated into the selvedge. As always, it is worth pointing out that the experiments were all done on real crystals that have a small number of steps and defects, rather than the perfect crystal models used in the calculations. For even larger doses of O_2 or NO_2, O becomes incorporated below the first layer of Rh. At Θ_O = 2 ML, the resulting structure is an O−Rh−O trilayer.[24,25] This is the most likely state for the results to be presented.[24] Ganduglia-Pirovano et al. predict that for Θ_O < 2 ML the subsurface oxygen forms (1×1) islands.[23] It is important to note that for all of these structures the surface O occupies hollow sites.

The CO + O reaction occurs via a Langmuir−Hinshelwood mechanism;[6,26] both O and CO are adsorbed on the surface before reaction. Therefore, it is important to understand where on the surface the CO is adsorbed and how significant is the bias toward a particular adsorption site. Thus far, most of the experimental measurements have been made at room temperature or below.[16,27−29] These involved either 0.25 or 0.5 ML of preadsorbed O, and the consensus is that, at least for low CO coverages, the CO adsorbs at on-top sites. Theoretical calculations further support this binding geometry.[29−31] As the CO coverage increases, however, it can move from on-top sites and into bridge and hollow sites. For instance, Schoiswohl et al.[28] have some CO adsorbed at hollow sites when Θ_O = 0.25 ML and Θ_{CO} = 0.5 ML.

Information about the dynamics of surface-catalyzed reactions can be obtained from the intensity and translational energy of the desorbing products, as reviewed by Kislyuk.[32] Two studies specifically investigated the dynamics of CO oxidation on Rh(111) surfaces by measuring the desorbing CO_2 product. A temperature-programmed reaction (TPR) study by Matsushima et al.[33] examined the angle-resolved intensity of desorbing CO_2 after exposure of the cold (100 K) Rh(111) surface to CO and O_2. In these experiments, the O dose was low (1.4 langmuirs), and with a 100 K surface, the coverage could never have been above 0.5 ML and probably less.[19] They did not measure the translational or internal energies of the desorbing CO_2 but did find that the intensity was sharply peaked toward normal. The Sibener group looked at the angle-resolved desorption and translational kinetic energy of the CO_2 product.[12,13] This was done under steady-state conditions and elevated surface temperatures (T_S = 475−1000 K). The results showed a bimodal energy distribution, with an intensity distribution having an angular dependence of the form $a \cos^n(\theta) + (1 - a) \cos(\theta)$, where θ is the scattering angle. The thermalized portion ($\langle E \rangle = 2k_B T_S$, where k_B is Boltzmann's constant) had a characteristic $\cos(\theta)$ intensity distribution. The second component was described by a $\cos^n(\theta)$ intensity distribution with $n \approx 9$ and had an average translational energy several times greater than thermal. At higher T_S, the translational energy of the desorbing CO_2 concomitantly increased, with a slope of $\sim 8.7 k_B T_S$ for $T_S \leq$ 700 K.[12] The prefactor a also increased with increasing T_S.

As mentioned, one problem with steady-state experiments under UHV conditions is that there can be a limit on the reactant coverages that can be attained, at most Θ_O = 0.3 ML for the Colonell et al. experiments.[12] As described earlier, we expect that all of the O was adsorbed. In the experiments to be described, we initially loaded the surface with O and then exposed it to CO. This allowed us to measure dynamical parameters under conditions of much higher Θ_O, including measurements where there was both ad- and absorbed O.

EXPERIMENTAL SECTION

These experiments were done in a UHV scattering chamber, base pressure 2×10^{-10} Torr. Up to three molecular beams could overlap on the target crystal. Any molecules that left the surface could be detected by a rotatable and differentially pumped quadrupole mass spectrometer (angular resolution of ∼1°). Translational energies were determined by time-of-flight (TOF) measurements, using a rotating chopper wheel that passed or blocked molecules with a pseudorandom pattern of slots. This cross-correlation technique allowed for a 50% duty cycle, which resulted in robust counting statistics.

The experiments were performed using a Rh(111) single crystal that was cut to within 1° of the (111) face, as determined by Laue X-ray backscattering. The crystal was welded to a manipulator which allowed for resistive heating. The sample was cleaned by a combination of Ar^+ bombardment and O_2 exposure at 900 K. Annealing of the surface was done at ∼1250 K. For normal cleaning during the course of these experiments, it was only necessary to use the O_2 exposure at 900 K, followed by a 3 min anneal at ∼1250 K. Cleanliness and surface order were determined by Auger electron spectroscopy (AES) and He atom scattering.

The molecular beams were formed by expanding ∼150 Torr of the pure gas (O_2 or CO) through a 200 μm pinhole orifice in the source vacuum chamber. The beams passed through three regions of differential pumping before entering the UHV scattering chamber and could be blocked with beam flags in the second differential pumping region. No attempt was made to characterize these beams, though from previous experience making beams under similar conditions, the flux was on the order of 0.1 ML/s, and the average translational energy was 80−90 meV with a very large spread of velocities.

The key to these experiments is preparing the Rh(111) surface with varying amounts of oxygen on the surface and in the selvedge. For lower Θ_O, this is easily done at elevated T_S (450−600 K). For example, only a 5 min exposure at T_S = 450 K is required to produce a half-monolayer of adsorbed O. Once the full half-monolayer O coverage is achieved, the reaction of O_2 with the surface is very slow, even at T_S = 600 K.[19] Much quicker is the use of NO_2,[19] at either 525 or 600 K. After O dosing, the crystal was then cooled to 450 K before being exposed to CO.

A surface temperature of 450 K was chosen because the rate of CO_2 evolution was greater than at more elevated temperatures. This was determined by isothermal titration experiments, where the total CO signal was collected during successive 5 s intervals; examples are shown in Figure 1. At least for Θ_O = 0.5 ML, as the surface temperature increased, the rate

dx.doi.org/10.1021/jp504369z | J. Phys. Chem. C 2014, 118, 14977−14982

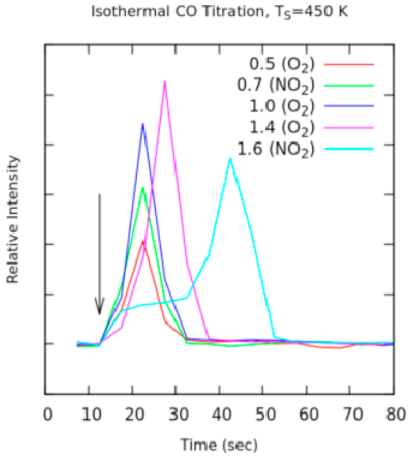

Figure 1. CO_2 signal from CO titration experiments for various Θ_O adsorbed on and absorbed into the Rh(111) surface. The surface was first dosed with the indicated reagent (T_S = 450 or 600 K for O_2 and 525 K for the NO_2) and then cooled to 450 K. The CO_2 signal was collected in 5 s increments, and the start of the CO exposure is indicated by the arrow.

at which the CO_2 was produced decreased; CO_2 production continued for a longer time interval, and so the intensity and signal-to-noise ratio were lower. This T_S also closely corresponded to the lowest temperature studied in the steady-state experiments.[12]

CO_2 translational velocities were measured by starting the TOF data collection and immediately opening the flag blocking the CO beam. The data collection time was determined by the results of the isothermal titration experiments and was usually 80 s. The detector had a large m/e = 44 signal, so ^{13}CO was used to improve the statistics, and several identical experiments were run and the data added for the final result. Representative TOF spectra, deconvolved from the cross-correlation pattern, are shown in Figure 2, along with a fit to the data from the largest Θ_O (1.6 ML). The fit is from a nonlinear least-squares program using the sum of two shifted Maxwell–Boltzmann velocity distributions

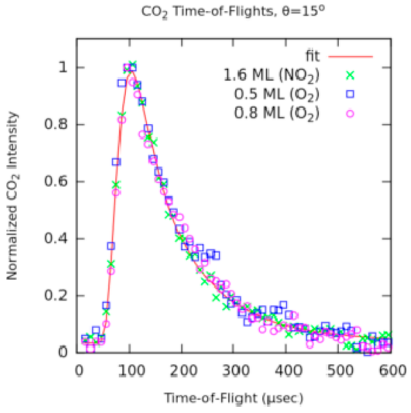

Figure 2. Example TOF spectra (deconvolved for the cross-correlaton pattern) for $^{13}CO_2$ produced by exposure of a 450 K Rh(111) surface to ^{13}CO after the indicated amount of O was adsorbed and absorbed. The fit (solid line) is for the initial Θ_O = 1.6 ML. The intensities have been adjusted so that the maximum for each of the spectra has the same value.

$$f(v) = A_1 v^3 \exp\left(-\left(\frac{v - v_1}{s_1}\right)^2\right) + A_2 v^3 \exp\left(-\left(\frac{v - v_2}{s_2}\right)^2\right) \quad (1)$$

where A_i, v_i, and s_i are all fitting parameters. The choice of fitting function is somewhat arbitrary, so the individual parameters may not have any good physical meaning. However, the fit is good and gives us a probability distribution with which to calculate the average energy as well as the integrated intensity. After exposure to the CO beam, there was no oxygen left on, or in, the Rh(111), as verified with AES.[33]

Since no O remains after CO exposure, the total oxygen coverage was determined by the CO_2 yield. The integrated CO_2 signal was referenced to that from Θ_O = 0.5 ML. A half-monolayer coverage of O was easily attained with a few minute exposure of O_2 at T_S = 450 K.[19] That there was a half-monolayer could be confirmed with He atom scattering (the (2 × 1)-O coverage gives a distinct diffraction pattern) and an absence of the low-temperature peak in the thermal desorption spectrum.[34]

RESULTS AND DISCUSSION

Figure 3 shows the total average translational kinetic energy, $\langle E_T \rangle$, as a function of θ, and Figure 4 shows the total intensity

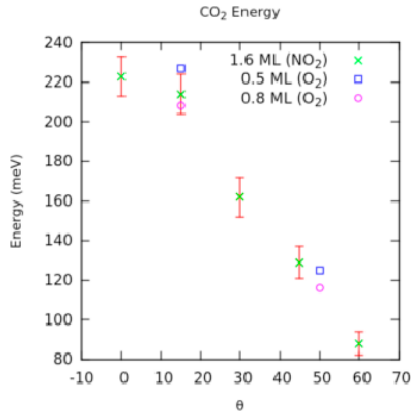

Figure 3. Total average translational energy ($\langle E_T \rangle$) of $^{13}CO_2$ as a function of θ and Θ_O. The different data sets are labeled by Θ_O and reagent.

as a function of θ. Obviously, there was more signal for Θ_O = 1.6 ML, and the dosing only took 10 min at T_S = 525 K. And since there is ample subsurface oxygen present, this is the coverage for which we took the most data. However, in Figure 3 there are also some results for Θ_O = 0.5 and 0.8 ML from O_2 dosing. Within the precision of our measurements, the results are identical for 0.5 ML ≤ Θ_O ≤ 1.6 ML.

In Figure 4, just the data for Θ_O = 1.6 ML are plotted. The line through the points is a least-squares fit to $I_T = a \cos^n(\theta) + (1 - a) \cos(\theta)$, with a = 0.6 and n = 8.6. As mentioned, the spectra were fit to two arbitrary Maxwell–Boltzmann distributions. However, the normal assumption of the angular intensity model is that the $\cos(\theta)$ term is due to molecules equilibrated to T_S with $\langle E_E \rangle = 2k_B T_S$ and $v_i = 0$.[32] This was the approach used our steady-state experiments[12] but led to a modification of the velocity distribution for the fast molecules. For a comparison to the previous paper, we simply extracted the average energy of the fast component, $\langle E_F \rangle$, assuming that the $\cos(\theta)$ distributed component was thermalized with the

dx.doi.org/10.1021/jp504369z | J. Phys. Chem. C 2014, 118, 14977–14982

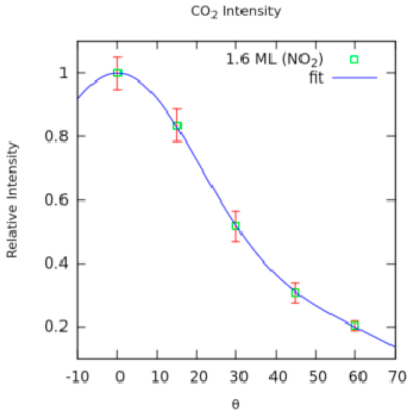

Figure 4. Angular dependence of the intensity (I_T) of $^{13}CO_2$ for Θ_O = 1.6 ML. The line is a fit to $I_T = a\cos^n(\theta) + (1 - a)\cos(\theta)$, with a = 0.6 and n = 8.6.

surface, $I_T = a\cos^n(\theta) + (1 - a)\cos(\theta) = I_F + I_E$, and $\langle E_T\rangle = (\langle E_F\rangle I_F + \langle E_E\rangle I_E)/I_T$. Using T =450 K and $\langle E_E\rangle$ = 77.55 meV, $\langle E_F\rangle \simeq$ 320 meV for $\theta \leq 30°$.

During the course of these experiments, the oxygen coverage was decreasing throughout the duration of the CO exposure. Thus, the observed CO_2 evolution was integrated over a continuum of Θ_O. However, the results for the average energy shown in Figure 3 would argue that this does not make much difference, at least for 0.5 ML $\leq \Theta_O \leq$ 1.6 ML. (Though not shown, the intensity ratios between θ = 15° and 50° at Θ_O = 0.5 and 0.8 ML are also consistent with the high coverage results shown in Figure 4.) For the steady-state experiments examined in Colonell et al.,[12] the prefactor (a) in the angular distribution of CO_2 intensity showed a strong T_S dependence, going from ~0.6 at T_S = 475 K to ~0.8 at 800 K.[12,13] We found that a = 0.6 at T_S = 450 K, consistent with the low T_S results. As for the average energy of the fast component ($\langle E_F\rangle$) at near normal θ, we found it to be significantly higher (320 meV) than the steady state results for T_S = 475 K and $\Theta_O \leq$ 0.3 ML. However, it fits in with the trend shown in Colonell[12] (Figure 10) that $\langle E_F\rangle$ increases with increasing Θ_O, going from ~210 meV at Θ_O = 0.1 ML to ~240 meV at Θ_O = 0.3 ML.

Interestingly, the surface coverage of oxygen atoms appears to have little effect on the energy or angular distribution of the CO_2 product. There is remarkable agreement between the results of the previous study[12] conducted at low oxygen coverage to those gathered here at much higher total oxygen coverages. Also, as clearly shown in Figure 3, there seems to be no difference for 0.5 ML $\leq \Theta_O \leq$ 1.6 ML, which spans a coverage range from all adsorbed to at least 0.6 ML absorbed. Another aspect of the surface warrants discussion, and that is the alteration of the rhodium oxidation state in the presence of high oxygen coverage on the surface and in the selvedge. At the temperature and pressure of our dosing ($T_S \leq$600 K and pressure at the surface ~10^{-7} Torr), the higher Θ_O coverage was probably in the form of the O−Rh−O trilayer.[23,24,35] For Θ_O < 2.0 ML, the adsorbed layer is complete, and the partial absorbed layer possibly forms subsurface islands.[23] The dynamics are consistent with the adsorption sites discussed in the Introduction. At 450 K, the Θ_{CO} is low, probably much less than a monolayer, since the flux is low and the desorption rate is high on either clean Rh(111)[36] or coadsorbed with O.[33] As discussed in the Introduction, the O occupies hollow sites and the CO tends to occupy atop sites. The O adsorbed on a hollow site reacts with a CO on a neighboring atop site, leading to a bent transition state geometry.[37] As surface O is reacted off, the subsurface O moves to the surface and takes its place. It is important to note that subsurface O appears to simply act as a reservoir to replenish surface O. This is in contrast to H reacting with hydrocarbons on Ni, where it is the subsurface atoms that are the reactive species.[38,39]

It is also worth noting the differences in the results of the titration experiments (Figure 1). For $\Theta_O \leq$ 1.0 ML, the CO_2 peaks occur promptly regardless of which reagent (O_2 or NO_2) was used. For the higher coverages, there is some lag in the CO_2 production. This is much more noticeable for the results with NO_2 dosing. For the experiments using NO_2 shown in the figures, exposure was done at T_S = 525 K. When the NO_2 exposure was done at T_S = 600 K, the results were similar, with slightly more CO_2 being produced, presumably because slightly more O was absorbed. At T_S = 600 K, any N or NO from NO_2 decomposition should definitely be desorbed.[40] It was suggested by Lundgren et al.[41] that the CO only sticks to steps or defects on the O−Rh−O surface. This leads to a slow rate at the beginning of the CO exposure, increasing as areas where the subsurface O has been depleted increase. If the CO can stick and react on areas where O is only adsorbed, or on defects in, or the edges of, O−Rh−O islands, the result would be slower initial reaction rates for larger initial Θ_O. Although there appear to be differences in the rates, the energy and angular distribution of the CO_2 product was not affected. Simulations of potential energy landscapes and rate processes for the coverage dependent surface and subsurface reaction pathways described in this paper for Rh(111), in a similar vein to recent work on metallic (100) surfaces,[42] would further enrich these findings.

CONCLUSIONS

In this paper, we described experiments where we measured the translational energy and angular intensity dependence of CO_2 produced from the reaction of CO with Rh(111) having 0.5 ML $\leq \Theta_O \leq$ 1.6 ML at T_S = 450 K. This spans coverages that have only absorbed O to ad- and absorbed O. The CO translational energy is independent of Θ_O. It is higher than the steady-state experiments done by Colonell et al.,[12] which were done at lower O coverages, but follows the trend that higher Θ_O leads to faster CO_2. The angular dependence of the intensity fit well to the form $I = a\cos^n(\theta) + (1 - a)\cos(\theta)$, with a = 0.6 and n = 8.6. Again, this was consistent with the low T_S of the previous steady-state results. These observations point to a similar reaction geometry regardless of the Θ_O.

AUTHOR INFORMATION

Corresponding Author

*E-mail s-sibener@uchicago.edu, Tel 773-702-7193 (S.J.S.).

Present Address

D.R.K.: Department of Chemistry, Loyola University Chicago, Chicago, IL.

Notes

The authors declare no competing financial interest.

ACKNOWLEDGMENTS

This work was supported by the Office of Basic Energy Sciences, Office of Science, U.S. Department of Energy, Grant DE-SC0002583, with further support for this project also coming from the Air Force Office of Scientific Research Grant

FA9550-10-1-0219. Infrastructure support from the NSF-Materials Research Science and Engineering Center at The University of Chicago is also gratefully acknowledged.

REFERENCES

(1) Matsushima, T. Angle-Resolved Measurements of Product Desorption and Reaction Dynamics on Individual Sites. *Surf. Sci. Rep.* **2003**, *52*, 1−62.
(2) Matsushima, T. Surface Structural Information Carried by Desorbing Reaction Products. *Prog. Surf. Sci.* **2007**, *82*, 435−477.
(3) Matsushima, T.; Shobatake, K. Catalytic Reactions Studied by Angle-Resolved Product Desorption. In *Catalysis*; The Royal Society of Chemistry: London, 2011; Vol. *23*, pp 139−178.
(4) Gao, F.; McClure, S. M.; Cai, Y.; Gath, K. K.; Wang, Y.; Chen, M. S.; Guo, Q. L.; Goodman, D. W. CO Oxidation Trends on Pt-Group Metals from Ultrahigh Vacuum to near Atmospheric Pressures: A Combined in Situ PM-IRAS and Reaction Kinetics Study. *Surf. Sci.* **2009**, *603*, 65−70.
(5) Gao, F.; Cai, Y.; Gath, K. K.; Wang, Y.; Chen, M. S.; Guo, Q. L.; Goodman, D. W. CO Oxidation on Pt-Group Metals from Ultrahigh Vacuum to Near Atmospheric Pressures. 1. Rhodium. *J. Phys. Chem. C* **2008**, *113*, 182−192.
(6) Gao, F.; Goodman, D. W. Reaction Kinetics and Polarization Modulation Infrared Reflection Absorption Spectroscopy Investigations of CO Oxidation over Planar Pt-Group Model Catalysts. *Langmuir* **2010**, *26*, 16540−16551.
(7) Hendriksen, B.; Bobaru, S.; Frenken, J. Looking at Heterogeneous Catalysis at Atmospheric Pressure Using Tunnel Vision. *Top. Catal.* **2005**, *36*, 43−54.
(8) Zhu, Z.; Tao, F.; Zheng, F.; Chang, R.; Li, Y.; Heinke, L.; Liu, Z.; Salmeron, M.; Somorjai, G. A. Formation of Nanometer-Sized Surface Platinum Oxide Clusters on a Stepped Pt(557) Single Crystal Surface Induced by Oxygen: A High-Pressure STM and Ambient-Pressure XPS Study. *Nano Lett.* **2012**, *12*, 1491−1497.
(9) Tao, F.; Tang, D.; Salmeron, M.; Somorjai, G. A. A New Scanning Tunneling Microscope Reactor Used for High-Pressure and High-Temperature Catalysis Studies. *Rev. Sci. Instrum.* **2008**, *79* (084101), 1−6.
(10) McClure, S. M.; Goodman, D. W. New Insights into Catalytic CO Oxidation on Pt-Group Metals at Elevated Pressures. *Chem. Phys. Lett.* **2009**, *469*, 1−13.
(11) Stoltze, P.; Nørskov, J. K. Bridging the "Pressure Gap" between Ultrahigh-Vacuum Surface Physics and High-Pressure Catalysis. *Phys. Rev. Lett.* **1985**, *55*, 2502−2505.
(12) Colonell, J. I.; Gibson, K. D.; Sibener, S. J. Carbon Monoxide Oxidation on Rh(111): Velocity and Angular Distributions of the CO_2 Product. *J. Chem. Phys.* **1995**, *103*, 6677−6690.
(13) Brown, L. S.; Sibener, S. J. A Molecular Beam Scattering Investigation of the Oxidation of CO on Rh(111). II. Angular and Velocity Distributions of the CO_2 Product. *J. Chem. Phys.* **1989**, *90*, 2807−2815.
(14) Wong, K. C.; Liu, W.; Mitchell, K. A. R. LEED Crystallographic Analysis for the Rh(111)-(2 × 1)-O Surface Structure. *Surf. Sci.* **1996**, *360*, 137−143.
(15) Schwegmann, S.; Over, H. Comment on "STM Study of Oxygen on Rh(111)" by H. Xu and K. Y. S. Ng. *Surf. Sci.* **1997**, *393*, 179−180.
(16) Schwegmann, S.; Over, H.; De Renzi, V.; Ertl, G. The Atomic Geometry of the O and CO + O Phases on Rh(111). *Surf. Sci.* **1997**, *375*, 91−106.
(17) Gibson, K. D.; Viste, M.; Sanchez, E.; Sibener, S. J. Physical and Chemical Properties of High Density Atomic Oxygen Overlayers under Ultrahigh Vacuum Conditions: (1 × 1)-O/Rh(111). *J. Chem. Phys.* **2000**, *112*, 2470−2478.
(18) Wider, J.; Greber, T.; Wetli, E.; Kreutz, T. J.; Schwaller, P.; Osterwalder, J. Direct Observation of Subsurface Oxygen on Rh(111). *Surf. Sci.* **1998**, *417*, 301−310.
(19) Peterlinz, K. A.; Sibener, S. J. Absorption, Adsorption, and Desorption Studies of the Oxygen/Rh(111) System Using O_2, NO, and NO_2. *J. Phys. Chem.* **1995**, *99*, 2817−2825.
(20) Castner, D. G.; Somorjai, G. A. LEED, AES and Thermal Desorption Studies of the Oxidation of the Rhodium(111) Surface. *Appl. Surf. Sci.* **1980**, *6*, 29−38.
(21) Köhler, L.; Kresse, G.; Schmid, M.; Lundgren, E.; Gustafson, J.; Mikkelsen, A.; Borg, M.; Yuhara, J.; Andersen, J. N.; Marsman, M.; et al. High-Coverage Oxygen Structures on Rh(111): Adsorbate Repulsion and Site Preference Is Not Enough. *Phys. Rev. Lett.* **2004**, *93* (266103), 1−4.
(22) Ganduglia-Pirovano, M. V.; Scheffler, M. Structural and Electronic Properties of Chemisorbed Oxygen on Rh(111). *Phys. Rev. B* **1999**, *59*, 15533−15543.
(23) Ganduglia-Pirovano, M.; Reuter, K.; Scheffler, M. Stability of Subsurface Oxygen at Rh(111). *Phys. Rev. B* **2002**, *65* (245426), 1−9.
(24) Gustafson, J.; Mikkelsen, A.; Borg, M.; Lundgren, E.; Köhler, L.; Kresse, G.; Schmid, M.; Varga, P.; Yuhara, J.; Torrelles, X.; et al. Self-Limited Growth of a Thin Oxide Layer on Rh(111). *Phys. Rev. Lett.* **2004**, *92* (126102), 1−4.
(25) Stampfl, C.; Soon, A.; Piccinin, S.; Shi, H.; Zhang, H. Bridging the Temperature and Pressure Gaps: Close-Packed Transition Metal Surfaces in an Oxygen Environment. *J. Phys.: Condens. Matter* **2008**, *20* (184021), 1−19.
(26) Schwartz, S. B.; Schmidt, L. D.; Fisher, G. B. Carbon Monoxide + Oxygen Reaction on rhodium(III): Steady-State Rates and Adsorbate Coverages. *J. Phys. Chem.* **1986**, *90*, 6194−6200.
(27) Jaworowski, A. J.; Beutler, A.; Strisland, F.; Nyholm, R.; Setlik, B.; Heskett, D.; Andersen, J. N. Adsorption Sites in O and CO Coadsorption Phases on Rh(111) Investigated by High-Resolution Core-Level Photoemission. *Surf. Sci.* **1999**, *431*, 33−41.
(28) Schoiswohl, J.; Eck, S.; Ramsey, M. G.; Andersen, J. N.; Surnev, S.; Netzer, F. P. Vanadium Oxide Nanostructures on Rh(111): Promotion Effect of CO Adsorption and Oxidation. *Surf. Sci.* **2005**, *580*, 122−136.
(29) Krenn, G.; Bako, I.; Schennach, R. CO Adsorption and CO and O Coadsorption on Rh(111) Studied by Reflection Absorption Infrared Spectroscopy and Density Functional Theory. *J. Chem. Phys.* **2006**, *124* (144703), 1−12.
(30) Kizilkaya, A. C.; Gracia, J. M.; Niemantsverdriet, J. W. A Direct Relation between Adsorbate Interactions, Configurations, and Reactivity: CO Oxidation on Rh(100) and Rh(111). *J. Phys. Chem. C* **2010**, *114*, 21672−21680.
(31) Zhang, A. H.; Zhu, J.; Duan, W. H. Oxidation of Carbon Monoxide on Rh(111): A Density Functional Theory Study. *J. Chem. Phys.* **2006**, *124* (234703), 1−4.
(32) Kislyuk, M. Desorption Dynamics of the Products of Heterogeneous Catalytic Reactions. *Kinet. Catal.* **2002**, *43*, 603−638.
(33) Matsushima, T.; Matsui, T.; Hashimoto, M. Kinetic Studies on the CO Oxidation on a Rh(111) Surface by Means of Angle-resolved Thermal Desorption. *J. Chem. Phys.* **1984**, *81*, 5151−5160.
(34) Gibson, K. D.; Viste, M.; Sanchez, E. C.; Sibener, S. J. High Density Adsorbed Oxygen on Rh(111) and Enhanced Routes to Metallic Oxidation Using Atomic Oxygen. *J. Chem. Phys.* **1999**, *110*, 2757−2760.
(35) Flege, J. I.; Sutter, P. In Situ Structural Imaging of CO Oxidation Catalysis on Oxidized Rh(111). *Phys. Rev. B* **2008**, *78* (153402), 1−3.
(36) Peterlinz, K. A.; Curtiss, T. J.; Sibener, S. J. Coverage Dependent Desorption Kinetics of CO from Rh(111) Using Time-resolved Specular Helium Scattering. *J. Chem. Phys.* **1991**, *95*, 6972−6985.
(37) Eichler, A. CO Oxidation on Transition Metal Surfaces: Reaction Rates from First Principles. *Surf. Sci.* **2002**, *498*, 314−320.
(38) Johnson, A. D.; Daley, S. P.; Utz, A. L.; Ceyer, S. T. The Chemistry of Bulk Hydrogen: Reaction of Hydrogen Embedded in Nickel with Adsorbed CH_3. *Science* **1992**, *257*, 223−225.
(39) Ceyer, S. T. The Unique Chemistry of Hydrogen beneath the Surface: Catalytic Hydrogenation of Hydrocarbons. *Acc. Chem. Res.* **2001**, *34*, 737−744.

(40) Jirsak, T.; Dvorak, J.; Rodriguez, J. Adsorption of NO_2 on Rh(111) and Pd/Rh(111): Photoemission Studies. *Surf. Sci.* **1999**, *436*, L683−L690.
(41) Lundgren, E.; Gustafson, J.; Resta, A.; Weissenrieder, J.; Mikkelsen, A.; Andersen, J. N.; Köhler, L.; Kresse, G.; Klikovits, J.; Biederman, A.; et al. The Surface Oxide as a Source of Oxygen on Rh(111). *J. Mol. Spectrosc.* **2005**, *144*−*147*, 367−372.
(42) Liu, D.-J.; Evans, J. W. Realistic Multisite Lattice-Gas Modeling and KMC Simulation of Catalytic Surface Reactions: Kinetics and Multiscale Spatial Behavior for CO-Oxidation on Metal (100) Surfaces. *Prog. Surf. Sci.* **2013**, *88*, 393−521.